

## A SEARCH FOR OPTICAL VARIABILITY OF TYPE 2 QUASARS IN SDSS STRIPE 82

AARON J. BARTH<sup>1</sup>, ALEXEY VOEVODKIN<sup>2,3</sup>, DANIEL J. CARSON<sup>1</sup>, PRZEMYSŁAW WOŹNIAK<sup>3</sup>

*Draft version June 25, 2018*

### ABSTRACT

Hundreds of Type 2 quasars have been identified in Sloan Digital Sky Survey (SDSS) data, and there is substantial evidence that they are generally galaxies with highly obscured central engines, in accord with unified models for active galactic nuclei (AGNs). A straightforward expectation of unified models is that highly obscured Type 2 AGNs should show little or no optical variability on timescales of days to years. As a test of this prediction, we have carried out a search for variability in Type 2 quasars in SDSS Stripe 82 using difference-imaging photometry. Starting with the Type 2 AGN catalogs of Zakamska et al. (2003) and Reyes et al. (2008), we find evidence of significant *g*-band variability in 17 out of 173 objects for which light curves could be measured from the Stripe 82 data. To determine the nature of this variability, we obtained new Keck spectropolarimetry observations for seven of these variable AGNs. The Keck data show that these objects have low continuum polarizations ( $p \lesssim 1\%$  in most cases) and all seven have broad  $H\alpha$  and/or Mg II emission lines in their total (unpolarized) spectra, indicating that they should actually be classified as Type 1 AGNs. We conclude that the primary reason variability is found in the SDSS-selected Type 2 AGN samples is that these samples contain a small fraction of Type 1 AGNs as contaminants, and it is not necessary to invoke more exotic possible explanations such as a population of “naked” or unobscured Type 2 quasars. Aside from misclassified Type 1 objects, the Type 2 quasars do not generally show detectable optical variability over the duration of the Stripe 82 survey.

*Subject headings:* galaxies: active — galaxies: nuclei — galaxies: photometry — quasars: general — polarization

### 1. INTRODUCTION

Unified models of active galactic nuclei (AGNs) have been extremely successful at explaining the different appearance of Type 1 (broad-lined) AGNs and Type 2 AGNs (those lacking broad emission lines) as resulting from anisotropic obscuration in a dusty torus surrounding the AGN’s central engine and broad-line region (BLR). The simplest version of the unified model (Antonucci 1993) posits that all Type 2 AGNs contain a hidden Type 1 nucleus that is obscured along our line of sight by a toroidal dust distribution. A broad range of observational evidence supports the general picture of toroidal obscuration regions in AGNs, including detection of “hidden” broad emission lines seen in polarized scattered light (Antonucci & Miller 1985), high X-ray obscuring columns in many Type 2 Seyferts (Mulchaey et al. 1992), and ionization cones in the narrow-line regions of Seyfert 2 galaxies (Pogge 1988). Recent work has suggested that orientation alone is probably insufficient to explain all of the differences between Type 1 and Type 2 AGNs, and in particular, the distribution of dust torus covering factors may be different for Type 1 and Type 2 samples (Ramos Almeida et al. 2011; Elitzur 2012). Nevertheless, even if the Type 1/2 dichotomy is not purely the result of orientation differences, it is firmly established that many Type 2 AGNs do contain a hidden Type 1 nucleus. For samples of Seyfert 2 galaxies at low redshift, the fraction found to contain hidden broad-line regions in polarized light is between  $\sim 35\%$  and  $50\%$  (Moran et al. 2000; Tran 2001).

The Sloan Digital Sky Survey (SDSS; York et al. 2000) provided the first opportunity for identification of large num-

bers of optically-selected Type 2 quasars. Zakamska et al. (2003, hereinafter Z03) carried out the first systematic search using SDSS Data Release 1 (DR1; Abazajian et al. 2003), and identified 291 Type 2 AGNs of which about half had [O III] luminosities above  $3 \times 10^8 L_{\odot}$ , placing them in the same luminosity range as quasars. Extending this work further using SDSS DR6, Reyes et al. (2008, hereinafter R08) used slightly modified selection criteria to compile a sample of 887 Type 2 AGNs all with [O III] luminosities above  $2 \times 10^8 L_{\odot}$ , and identified these as Type 2 counterparts of luminous quasars. Follow-up X-ray observations demonstrated that many of these objects are moderately to highly absorbed (Zakamska et al. 2004; Vignali et al. 2004, 2006; Jia et al. 2012), and Zakamska et al. (2005) found evidence of high optical continuum polarization and polarized broad emission lines in several objects. Such properties support the identification of these objects as obscured Type 2 versions of quasars.

Temporal variability is one of the hallmarks of AGN activity, but for highly obscured AGNs the unified model would predict that optical variability should be highly suppressed since the observer’s line of sight to the central continuum source and broad-line region is blocked by the dusty torus. Even if some AGN continuum emission was visible in scattered light, the dominant and non-variable contribution of host galaxy starlight would strongly dilute the variability of the scattered AGN light. Additionally, any variability in the scattered light component would be temporally blurred by reflection from a spatially extended scattering region, so that short-term flux variations on timescales shorter than the light-crossing time across the scattering region would tend to be smoothed out. Given these considerations, optical variability of Type 2 AGNs has seldom been investigated, although some variability surveys have identified a small number of

<sup>1</sup> Department of Physics and Astronomy, 4129 Frederick Reines Hall, University of California, Irvine, CA, 92697-4575, USA; barth@uci.edu

<sup>2</sup> Space Research Institute (IKI), Profsoyuznaya 84/32, Moscow, Russia, 117997

<sup>3</sup> Los Alamos National Laboratory, MS-D466, Los Alamos, NM, 87545

candidate variable Type 2 AGNs (e.g., Bershadsky et al. 1998; Sarajedini et al. 2006). Yip et al. (2009) carried out the largest systematic investigation of Type 2 AGN variability to date. They used SDSS spectroscopic data to search for variability in the subset of AGNs having two epochs of spectroscopy, and found no evidence of continuum or emission-line variability in Type 2 AGNs on timescales of months to a few years.

One intriguing result comes from a long-term monitoring program by Hawkins (2004). In a 25-year photographic survey, Hawkins (2004) found evidence of optical flux variations in some AGNs which had spectra consistent with a Type 2 classification. Overall, 10% of the emission-line galaxies in the Hawkins (2004) survey were found to be Type 2 AGNs showing significant flux variability. Hawkins’ interpretation was that these objects do not conform to the standard unified model. He proposed that these are narrow-lined AGNs that are *not* obscured and which do not possess broad-line regions at all, i.e., “naked AGNs” in which the central engine is unobscured. While plausible candidates for naked Type 2 nuclei (sometimes elsewhere referred to as “true” Type 2 AGNs) have been identified at very low luminosities in nearby galaxies (e.g., Pappa et al. 2001; Shi et al. 2010; Tran et al. 2011), it would be surprising if such objects, totally lacking a BLR, were common at high luminosity. (See Antonucci 2012 for a critique of “true” Type 2 AGN classification.)

The SDSS Stripe 82 database has enabled a variety of new investigations of AGN variability. Stripe 82 data has been used extensively to examine continuum variability in quasars (Sesar et al. 2007; Bhatti et al. 2010; Ai et al. 2010; MacLeod et al. 2010; Meusinger et al. 2011; Gu & Ai 2011; Sakata et al. 2011; Voevodkin 2011; Schmidt et al. 2012; MacLeod et al. 2012; Zuo et al. 2012) and to develop new methods for quasar selection by variability (Schmidt et al. 2010; MacLeod et al. 2011; Butler & Bloom 2011; Palanque-Delabrouille et al. 2011; Wu et al. 2011), but Type 2 quasar variability in Stripe 82 has not previously been examined. The combination of the Z03 and R08 samples together with the Stripe 82 data archive provides an opportunity to investigate the photometric variability of a substantial sample of Type 2 quasars over a duration of nearly a decade. While there are now extensive samples of obscured high-luminosity AGNs selected from infrared and X-ray surveys, the SDSS-selected Type 2 quasars are particularly well suited to examination of optical variability because of their relatively bright optical magnitudes and the large number ( $> 200$ ) that are located in the Stripe 82 survey area.

In this paper, we describe a new search for variability in luminous Type 2 AGNs in Stripe 82 using image-subtraction photometry, and follow-up observations to examine the nature of the variable sources. The methods for identification of variable AGNs are described in Section 2, along with illustrations of the light curves and spectra of the selected objects. Section 3 describes new Keck Observatory spectropolarimetry observations of seven objects. Section 4 describes properties of the individual objects, and in Section 5 we discuss the possible causes of variability in these objects. We find that over the duration of the Stripe 82 survey, the majority of the Type 2 quasars do not show any evidence of optical variability, consistent with straightforward expectations from the unified model. However, about 10% of previously identified Type 2 AGNs in Stripe 82 do exhibit significant flux variations. Examination of the SDSS spectra and our new Keck observations suggests that most of the variable objects are in fact Type 1 AGNs that were previously classified as

Type 2 objects either due to low S/N in the SDSS data, lack of sufficient wavelength coverage to detect broad H $\alpha$  or Mg II in the SDSS spectra, or other spectral peculiarities that rendered the classification ambiguous. Some appear to be variable intermediate-type (1.8/1.9) AGNs or narrow-line Seyfert 1 galaxies with properties similar to previously known examples of Type 2 quasar impostors. We cannot rule out the possibility that some objects identified in our search may be genuinely variable Type 2 AGNs, but such objects, if they exist at all, must be very rare.

## 2. DATA AND MEASUREMENTS

### 2.1. Sample Selection

We base our study on the Type 2 AGN samples of Z03 and R08. The samples were compiled using SDSS Data Release 1 (DR1; Abazajian et al. 2003) and Data Release 6 (DR6; Adelman-McCarthy et al. 2008) spectroscopic data, respectively. We briefly summarize the selection criteria of the two samples, and refer the reader to Z03 and R08 for full descriptions of the sample selection methodology. The Z03 sample includes objects in the redshift range  $0.3 < z < 0.83$  having narrow emission lines with ratios consistent with a high-ionization AGN classification and no detectable broad-line components. Z03 identified 291 Type 2 AGNs, with [O III]  $\lambda 5007$  luminosities spanning a broad range from  $\sim 10^7$  to  $10^{10} L_{\odot}$ . About half of the sample has  $L([\text{O III}]) > 3 \times 10^8 L_{\odot}$ , and these objects can be identified as luminous Type 2 quasars. In the R08 catalog, Type 2 quasars were selected based on slightly modified criteria: redshifts  $z < 0.83$  were selected (with no minimum redshift), a luminosity threshold of  $L([\text{O III}]) > 10^{8.3} L_{\odot}$  was applied in order to exclude AGNs of lower luminosity (i.e., Seyfert 2 galaxies), and a modified method was used to exclude objects showing broad components on the Balmer emission lines. Furthermore, the [O III] line was required to have an equivalent width  $> 4 \text{ \AA}$  and a S/N sufficient for a clear AGN classification. For objects above the [O III] luminosity threshold, R08 recover the selection of  $> 90\%$  of DR1 objects that were previously identified by Z03. Those objects in the Z03 catalog which are not in the R08 catalog are either below the minimum [O III] luminosity to be included, or they have low-S/N spectra or could not be classified unambiguously as AGN.

A substantial fraction of these Type 2 quasars are found in the Stripe 82 region, enabling us to examine their light curves over a  $\sim 9$ -year duration. Stripe 82 covers a strip of sky along the celestial equator in the region  $-60^{\circ} \leq \alpha \leq 60^{\circ}$  and  $-1.25^{\circ} \leq \delta \leq 1.25^{\circ}$  (Adelman-McCarthy et al. 2008). The observations of the Stripe 82 field started on 1998 September 19 and continued each fall during a 2–3 month period. The median number of observations per field is about 70, and the last 5 years of the light curves are more densely sampled than the initial years. The Stripe 82 region contains 110 Z03 AGNs and 143 R08 AGNs, respectively, with 45 objects in common between the two samples. Thus, we select 208 unique AGNs in Stripe 82 as our starting sample. For reasons described above, the R08 sample is expected to have a higher purity for selection of genuine Type 2 quasars than the Z03 sample, but for completeness, we start with the set of all of the Z03 and R08 objects located in Stripe 82 to examine their variability.

### 2.2. Analysis of Variability

Since the Type 2 AGNs are spatially extended sources and contain a substantial or dominant contribution of starlight

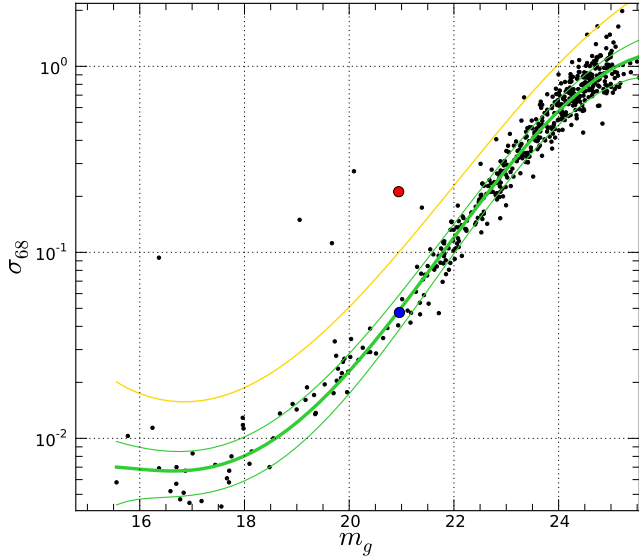


FIG. 1.— The quality of difference-image photometry for a typical field. Black points correspond to all sources detected in that field. The thick green line shows the median of the variability of the sources, and thin green lines show the  $1\sigma$  scatter around the median. The yellow line denotes the  $5\sigma$  threshold used to select variable sources. The large red data point represents one of the variable AGNs selected in this study, SDSS J033123, and the large blue point is a non-variable object having a similar median magnitude of  $m_g \approx 21$  mag. The light curves for these two sources are compared in Figure 2.

from the host galaxies, the standard SDSS catalog photometry is not optimal for detection of low-level variability. Given the expectation that any variable flux, if present at all, should be a weak and spatially compact component superposed on the extended host galaxy, an image-subtraction approach becomes very advantageous in this context. Our examination of the AGN light curves is based on difference image photometry (Alard & Lupton 1998) applied to the  $g$ -band Stripe 82 imaging database. The details of the procedure are described by Voevodkin (2011). One of its outputs is a set of high quality relative light curves for all sources in a given SDSS field.

The quality of photometry for a typical field is demonstrated in Figure 1. It shows the root-mean-square (rms) fluctuation level of the light curve (specifically, the 68th percentile of absolute deviations from the median,  $\sigma_{68}$ ) versus median magnitude for every source identified in that field. This includes both pointlike and extended objects, down to a detection limit that corresponds to a  $3\sigma$  threshold in a high-S/N reference image constructed by co-adding individual images with the best seeing. (The specific detection limit does not affect our results because all of the Z03 and R08 AGNs we examine are at least a few magnitudes brighter than this limit.) The vast majority of objects in the field are non-variable, and fall in a tight diagonal locus in which the increasing rms at faint magnitudes is the result of photometric uncertainties. Points that lie well above this locus are objects showing significant variability in their light curves. Figure 2 illustrates sample light curves for the two 21st-magnitude objects highlighted in Figure 1, one variable and one non-variable.

The data quality was sufficient to produce image-subtraction light curves for 173 of the 208 AGNs. The pipeline was unable to produce light curves for the remaining 35 AGNs for a variety of reasons, including locations close to the edges of images or close to very bright stars, a lack of suitable calibration stars, or a location in fields having fewer

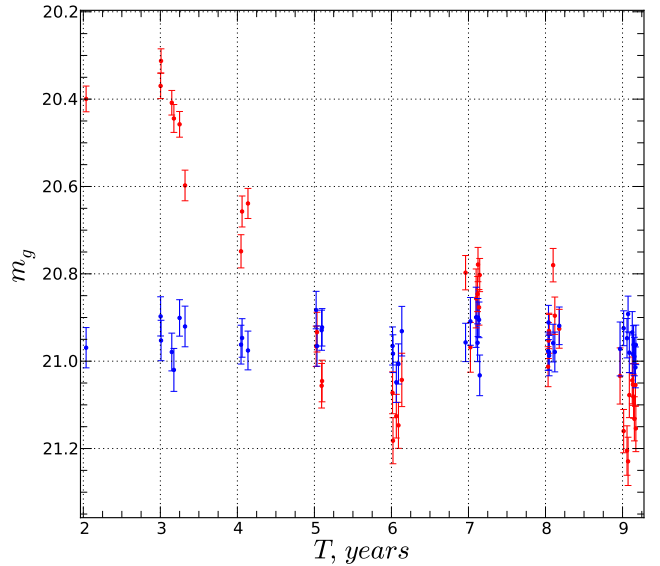


FIG. 2.— Light curves for the two objects represented by the red and blue points in Figure 1, illustrating variable and nonvariable objects at similar median magnitudes of  $m_g \approx 21$  mag. The zeropoint of the time axis corresponds to 1998 September 19.

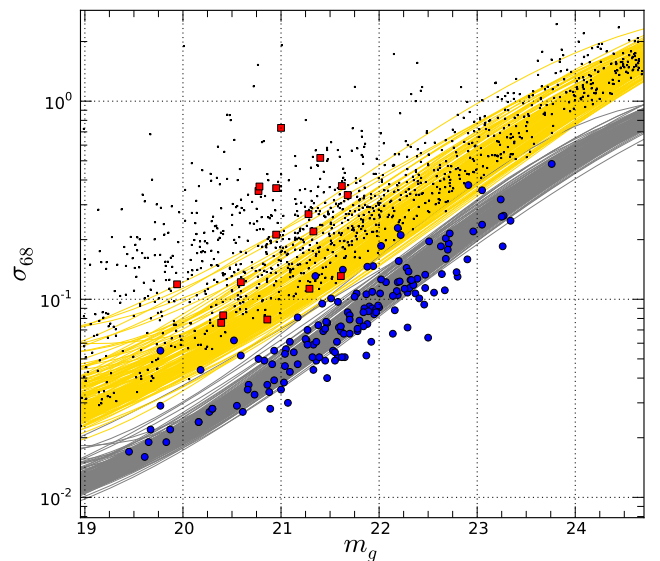


FIG. 3.— Variability selection for all Stripe 82 fields. Red squares and blue points correspond to Type 2 quasars lying above and below the variability threshold in their respective fields. The sets of gray and yellow lines show the median loci and  $5\sigma$  variability thresholds of all considered fields. Small black points represent all sources which lie above the variability threshold for their field.

than 20 suitable epochs of good-quality imaging. Of the 173 AGNs with light curves, 54 are from the Z03 sample only, 84 are from R08 only, and 35 are present in both samples. These 173 AGNs lie in 172 separate Stripe 82 fields, since one field contains two AGNs. The median number of points in the light curves is 36.

In order to identify variable AGNs, we require criteria to select objects having light curve variations significantly greater than the expected scatter due to photometric errors for non-variable objects of a given magnitude. We use the  $\sigma_{68}$  vs.  $m_g$  diagram (as in Figure 1) for each photometric field as the basis of our selection. The non-variable locus can be characterized by some function of magnitude and by the scatter around this

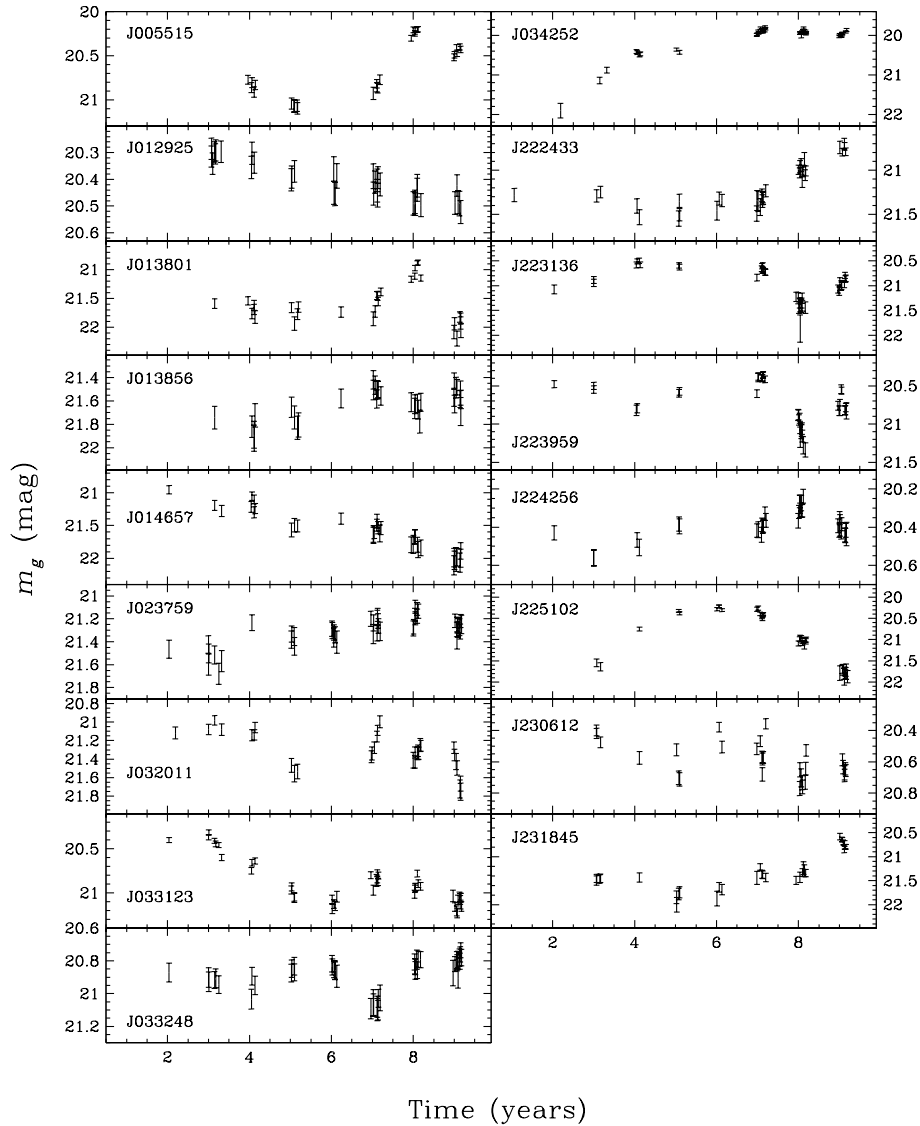


FIG. 4.— Light curves for the 17 variable objects.

function, where the scatter also depends on magnitude. To find an analytic approximation for the non-variable locus, we first calculated the median value of  $\sigma_{68}$  and its standard deviation over a running window containing 10 data points ranked in order of increasing  $m_g$ . Any  $2\sigma$  or greater outliers were then excluded and the median values were recalculated, producing a smoothed set of data points which were fit in log-log space by a 4th-order polynomial. This polynomial fit defines the non-variable locus illustrated with a thick green curve in Figure 1. To determine the  $1\sigma$  scatter band, we first flattened the data by subtracting the analytic approximation for the non-variable locus from the data points. Then, in the flattened data, we calculated the standard deviation of  $\sigma_{68}$  over a running boxcar containing 10 data points, producing a smoothed version of the scatter region. This set was then fitted with a 3rd-order polynomial in log-log space, and transformed back to the  $\sigma_{68}$  vs.  $m_g$  plane as illustrated in Figure 1 with thin

green curves.

Light curves of objects within and somewhat beyond the  $1\sigma$  scatter band appear non-variable within the measurement uncertainties, as shown for one sample object in Figure 2. The problem of identification of variable sources then becomes a question of selecting some appropriate threshold above the nonvariable locus. From examination of light curves from sources from several fields, we choose a threshold for selection of variable sources corresponding to a deviation of  $5\sigma$  above the non-variable locus. The  $5\sigma$  threshold is illustrated by the yellow curve in Figure 1. We apply this criterion to the fields containing all 173 Type 2 AGNs. In selecting this threshold, we have chosen to prioritize purity over completeness. In other words, visual examination of all light curves that exceed the  $5\sigma$  threshold confirms the presence of systematic flux variations that show some coherence over multiple observation dates, while the same is not true systematically

TABLE 1  
VARIABLE TYPE 2 AGN CANDIDATES

SDSS ID	$\alpha$	$\delta$	Sample	$z$	$m_g$ (mag)	$\sigma_{68}$ (mag)	$\log L([\text{O III}])/L_{\odot}$
J005515.81–004648.5	13.815917	–0.780167	Z	0.345	20.77	0.352	8.15
J012925.81–005900.2	22.357571	–0.983405	R	0.711	20.41	0.083	9.71
J013801.57–004946.5	24.506542	–0.829583	Z	0.433	21.68	0.336	8.29
J013856.14+003437.4	24.733919	+0.577056	Z	0.478	21.61	0.131	8.29
J014657.23+0055537.2	26.738502	+0.927000	Z	0.422	21.62	0.373	8.04
J023759.75+001723.5	39.499002	+0.289889	Z	0.335	21.29	0.113	7.46
J032011.94+002702.2	50.049792	+0.450611	Z	0.443	21.33	0.220	7.92
J033123.14–005930.7	52.846417	–0.991889	Z	0.431	20.95	0.212	9.05
J033248.49–001012.3	53.202095	–0.170094	Z+R	0.310	20.86	0.079	8.53
J034252.47+005252.4	55.718632	+0.881232	Z+R	0.565	19.94	0.119	8.93
J222433.31–003634.0	336.138824	–0.609475	R	0.588	21.28	0.269	8.87
J223136.27–011045.0	337.901126	–1.179167	Z	0.436	20.95	0.364	8.60
J223959.04+005138.3	339.996002	+0.860639	Z	0.384	20.78	0.371	8.15
J224256.47+005155.2	340.735382	+0.865334	R	0.410	20.39	0.076	9.26
J225102.40–000459.8	342.760000	–0.083306	Z	0.550	21.00	0.733	9.13
J230612.90–005912.6	346.553772	–0.986841	R	0.250	20.59	0.122	8.38
J231845.12–002951.4	349.688002	–0.497611	Z	0.397	21.40	0.517	8.00

NOTE. — We include both the sexagesimal and decimal coordinates (all J2000) to facilitate cross-matching with the original Z03 and R08 catalogs. The “Sample” column indicates whether an object is in the Z03 or R08 samples, or both. The listed  $g$ -band magnitudes represent the median magnitude over the Stripe 82 light curve. [O III] luminosities are taken from the Z03 and R08 catalogs. The SDSS sexagesimal designations are those listed in NED for each object, and we note that for some objects the right ascension and declination coordinates differ in the last decimal places from the object designations listed in Z03.

for lower selection thresholds. There are likely to be some genuinely variable objects that lie below the  $5\sigma$  cut due to a weaker level of variability, or variability affecting only a small portion of the light curve, so our sample of variable AGNs represents a lower limit to the total number of variable objects in the Z03 and R08 parent samples. The number of selected variable AGNs is not very sensitive to small changes in the detection threshold. If we change the threshold by  $\pm 0.3\sigma$  for example, the change in the number of selected variable sources is  $\pm 1$ .

Each field is analyzed separately, as the different photometric characteristics of the dataset for each field result in different locations for the non-variable locus and the  $5\sigma$  variability threshold. In particular, the location of the non-variable locus and the scatter of objects around it depend primarily on the mean seeing and the scatter in seeing for all of the observations of a given field. The overall picture of the variability selection is shown in Figure 3. In this figure, the non-variable locus and  $5\sigma$  threshold for each field are illustrated as gray and yellow curves, respectively. It is apparent that there is a wide range in the variability thresholds for different fields, due to the variations in image quality. Red squares show the Z03 and R08 AGNs lying above the  $5\sigma$  threshold for each field, and blue circles illustrate the AGNs falling below the  $5\sigma$  cut, while the small black points illustrate *all* detected sources that satisfy the variability selection in each field.

The majority of the Type 2 AGNs fall very close to the non-variable loci in the diagram, consistent with the general expectation that Type 2 AGNs should not be strongly variable in the optical. However, there are 17 objects from the Z03 and R08 catalogs which lie above the  $5\sigma$  thresholds for their respective fields. Their SDSS designations, redshifts, median magnitudes, rms variability amplitudes ( $\sigma_{68}$ ), and [O III] luminosities are given in Table 1 and we discuss their properties below. We find 13 variable AGNs from Z03 and 6 variables from R08, with two objects in common between the two samples. The light curves of the variable sources are displayed in Figure 4.

Our variability selection method based on rms brightness fluctuations allows detection of objects showing significant flux changes over and above the level expected from photometric measurement errors alone, but it gives no information about the timescale over which variations occur. The measured value of  $\sigma_{68}$  for an AGN depends on the underlying variability behavior, the cadence of observations, and the photometric quality of the images which sets the level of random measurement errors. Thus,  $\sigma_{68}$  combines variability information on all observed timescales and uses the full available information in the light curve to test for variability. By determining the variability threshold separately for each Stripe 82 field, each AGN is compared with other objects that were observed with the same cadence as well as identical observing conditions at each epoch; this provides a consistent framework for detection of variable sources despite the wide range in variability thresholds in different fields (Figure 3).

Figure 5 illustrates the SDSS spectra of the selected variable sources. Close examination of the spectra shows that many of them contain definite or possible broad emission lines in their spectra, primarily either  $H\alpha$  or Mg II. In some cases the identification of broad emission lines appears plausible but ambiguous, because  $H\alpha$  and Mg II appear at the noisy red or blue ends of the spectra. Among these 17 AGNs, one object is easily identified as a misclassified Type 1 quasar: J012925 (from the R08 sample) has broad  $H\beta$ ,  $H\gamma$ ,  $H\delta$ , and Mg II. It may have been misidentified as a Type 2 AGN in the R08 sample because it has a peculiar spectrum with unusually broad [O III] emission, in which the 4959 Å and 5007 Å lines are strongly blended. The individual spectra are described in Section 4. In most cases, a higher S/N spectrum would be needed to carry out a definitive test for broad-line emission, but even with only the SDSS spectra it appears plausible that some of these variable objects are actually Type 1 AGNs.

### 3. SPECTROPOLARIMETRY

In order to distinguish among possible explanations for the observed variability, we conducted new observations using the LRISp dual-beam spectropolarimeter (Oke et al. 1995;

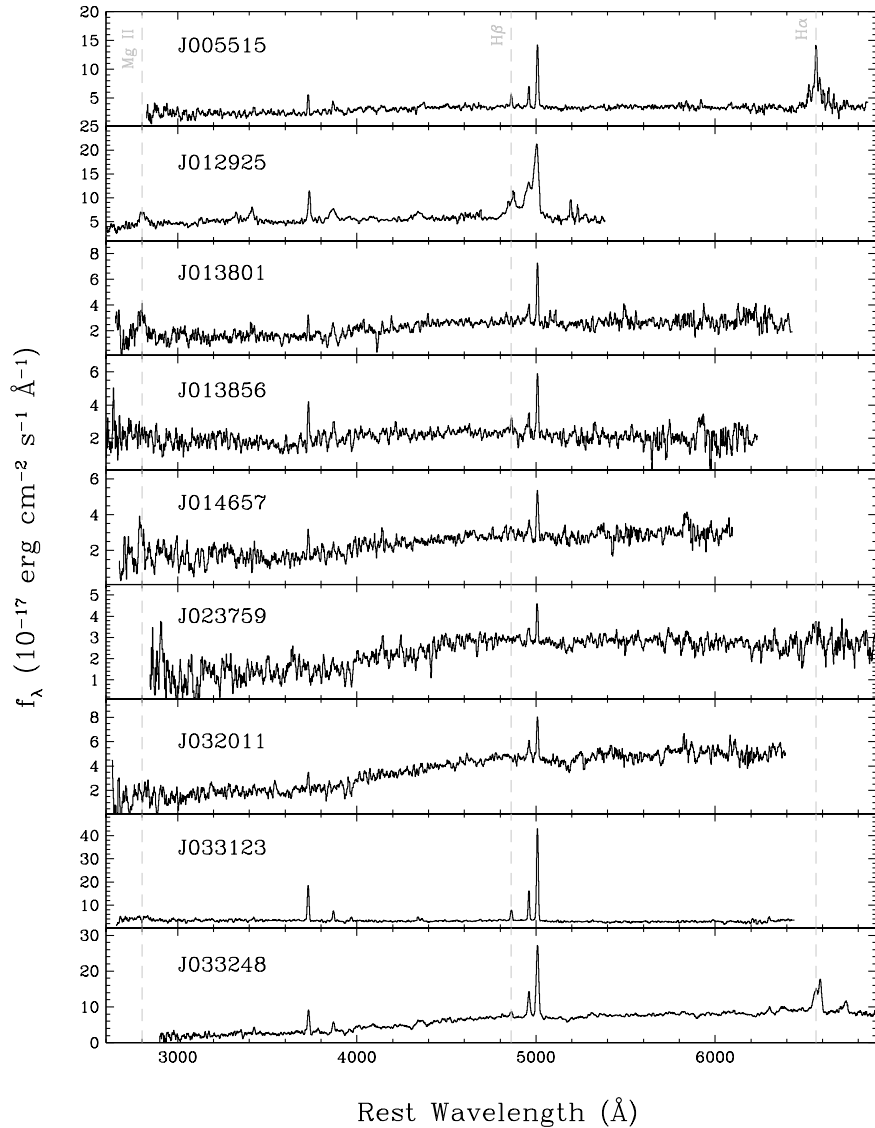


FIG. 5.— SDSS spectra of the variable AGNs. Data have been binned to  $2 \text{ \AA}$  per wavelength bin and smoothed with a 5-pixel boxcar.

Goodrich et al. 1995) at the Keck I telescope. With these observations, our aims were to test for the presence of broad emission lines in the total flux spectrum using spectra of broader wavelength coverage and higher S/N than the SDSS spectra, and to search for strongly polarized continua and/or polarized broad emission lines that could provide evidence for the existence of highly obscured nuclei seen only in scattered light. One possible outcome would be a measurement of low polarization, together with the detection of broad lines in total flux. This would imply that a target is actually a Type 1 AGN that was misclassified as a Type 2 object, or possibly that it underwent a state change due to a substantial change in line-of-sight obscuration since the SDSS spectrum was taken. Alternatively, a detection of highly polarized continuum and broad-line emission would indicate that the detected variability must be coming from the scattered light component, implying a very compact size (smaller than several light-years)

for the scattering region. If an object has low polarization and does not show broad lines in either total flux or polarized flux, it would remain a candidate for being a naked Type 2 quasar lacking a BLR, although additional evidence would be required in order to confirm this classification, such as measurement of the X-ray obscuring column density.

The LRISp observations were carried out during the night of 2012 September 20 UT in clear conditions, with seeing around  $1''$ . We used a  $1''$  slit width, and a D560 dichroic to separate the blue and red beams. The blue side of the spectrograph used a  $400 \text{ grooves mm}^{-1}$  grism and the red side used a  $400 \text{ grooves mm}^{-1}$  grating, giving dispersion of  $1.09 \text{ \AA/pixel}$  and  $1.16 \text{ \AA/pixel}$  on the blue and red sides, respectively. The total wavelength coverage for the combined blue and red sides was  $3100\text{--}10300 \text{ \AA}$ , with a small overlap at  $5600\text{--}5700 \text{ \AA}$ .

During the course of the night, we observed seven AGNs selected from the list described above. Each was observed in

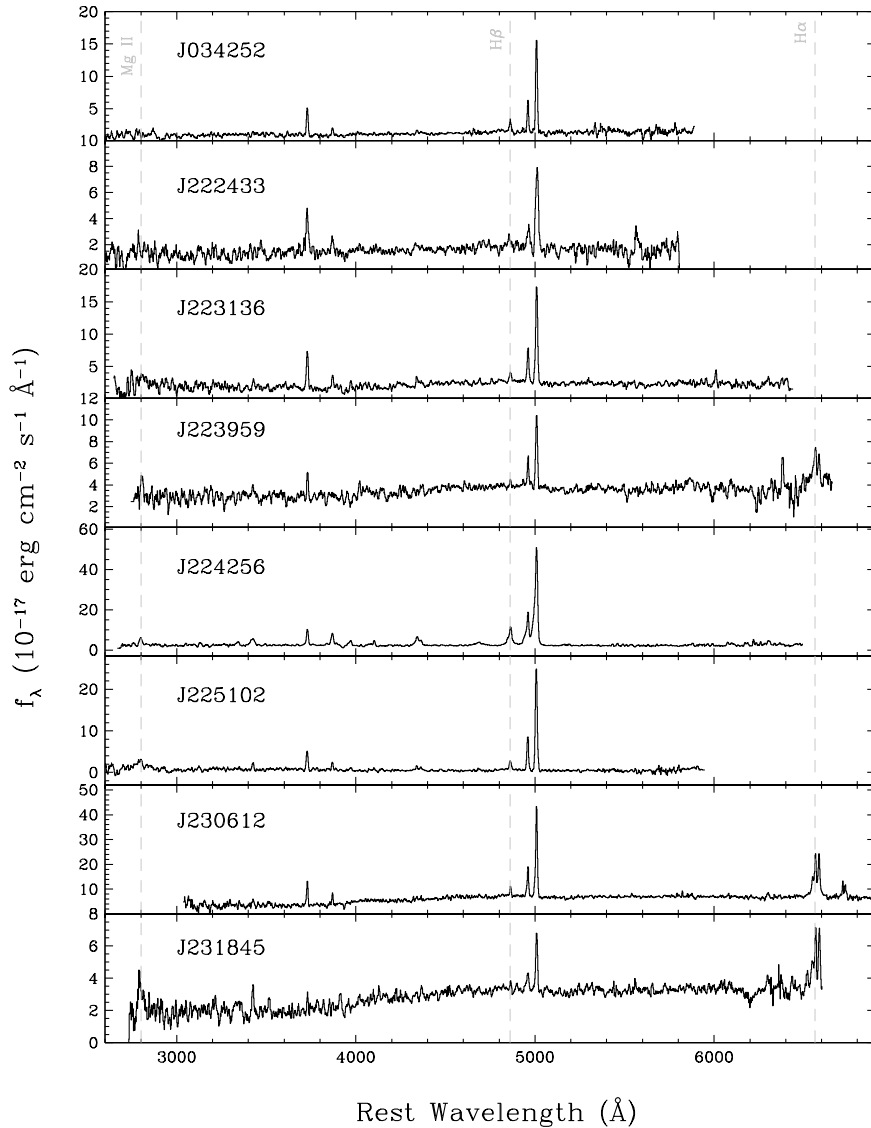


FIG. 5.— (Continued)

a standard sequence of four settings of the rotatable half-wave plate ( $0^\circ$ ,  $45^\circ$ ,  $22.5^\circ$ , and  $67.5^\circ$ ), with exposure times of 680 and 600 seconds for the blue and red exposures, respectively. Shorter exposure times were used for the red side to compensate for the longer readout time of the LRIS red CCDs. Each AGN was observed for one full observation sequence, for a total of 2720/2400 s (blue/red sides), except that for J224256 we obtained two exposure sequences. Additionally, we observed the null (unpolarized) star HD 154892, the polarized standards HD 155528 and HD 283812, and the flux standards BD +28°4211 and G191B2B. Data were reduced and calibrated following methods described by Miller et al. (1988) and Barth et al. (1999). Over the wavelength range 4500–5400 Å, the null standard star had  $p = (0.038 \pm 0.003)\%$ , indicating a negligible level of instrumental polarization.

For the polarization measurements described below, we use only the blue-side data. The red-side data are more impacted

by residuals from strong cosmic-ray hits in the LRIS red detectors, which are  $300 \mu\text{m}$ -thick LBNL CCDs (Rockosi et al. 2010). The high rate of cosmic-ray events limited the feasible exposure times to  $\sim 10$  minutes, which severely constrained the S/N achievable in a single exposure. Imperfect cleaning of the very large multi-pixel cosmic-ray hits on the red CCD left numerous small residuals that caused spurious features in the Stokes parameter spectra. These residuals are more severe for spectropolarimetry than for standard spectroscopy because the polarization calculation relies on measurement of the small flux differences between the orthogonally polarized beams. Additionally, during much of the night the spatial focus in the red camera was relatively poor and in some of the red-side exposures the spatial profile of the target was slightly bifurcated; this focus problem did not affect the blue camera. As a result, we were able to extract reasonable total-flux spectra for the red side, but the red polarization measurements

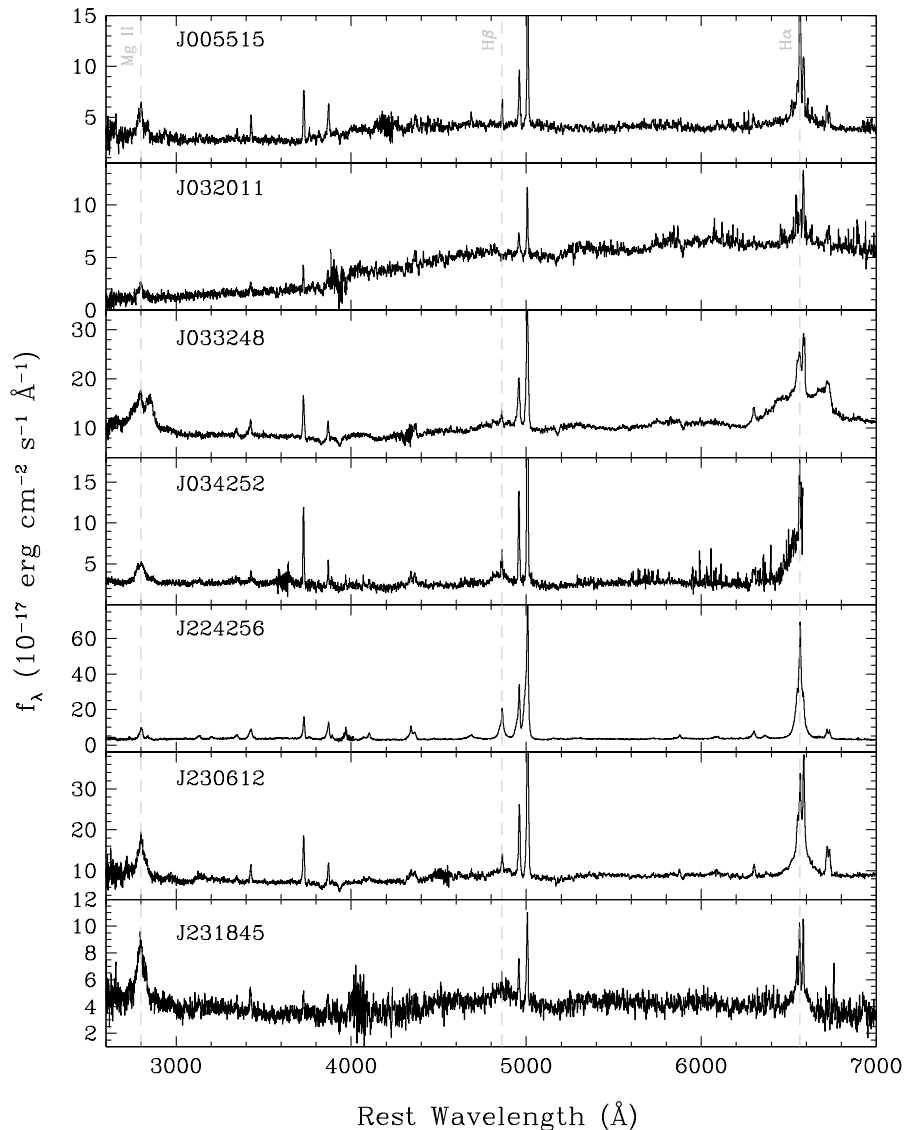


FIG. 6.— LRISp total-flux spectra of the seven AGNs observed at Keck. The noisy spectral region seen near 4000–4500 Å in some spectra corresponds to the dichroic cutoff at 5600 Å in the observed frame.

were not as reliable as the blue side data.

Figure 6 illustrates the LRISp total-flux spectra of these seven objects. The primary result that emerges from the LRISp spectra is that all seven of these objects have broad  $H\alpha$  and/or broad  $Mg\ II$  emission lines in total flux. These broad lines are fairly obvious in five of the seven objects: J005515, J033248, J034252, J230612, and J231845. In the case of J032011, the S/N in the LRISp spectrum is fairly low, but close examination clearly shows the  $Mg\ II$  and  $H\alpha$  lines to be much broader than  $[O\ III]\ \lambda 5007$ . The remaining AGN, J224256, has a spectrum which might appear superficially to be consistent with a Type 2 classification, but we find that it has broad  $Mg\ II$  emission as well as broad wings on  $H\alpha$  and  $H\beta$  that are not present on the forbidden  $[O\ II]$  and  $[O\ III]$  lines. Section 4 contains a more detailed discussion of the classification of this object and others. Given that our sample selection began with catalogs of Type 2 AGNs, it is a rather

striking result that *all* of the variable objects for which we have obtained new spectra show broad emission lines in their total flux spectra.

In no case do we see any evidence for features in the Stokes parameter spectra at the wavelengths of permitted emission lines, so we do not identify any examples of hidden broad line regions in this sample. We measured the continuum polarization of each object over a broad wavelength range on the blue side, selected for each object to exclude strong emission lines. Table 2 lists the continuum polarization measurements, as percent linear polarization and polarization angle  $\theta$ .

Four objects have continuum polarizations that are essentially consistent with zero, and two others have weak polarizations of about 1%. The only object in our sample with a polarization greater than 2% is J224256, with  $p = (2.39 \pm 0.37)\%$  over 4920–5320 Å. We did not observe interstellar probe stars

to measure the Galactic interstellar polarization (e.g., Tran 1995), so we cannot directly determine the Galactic contribution to the measured polarization. However, we can estimate the maximum expected value of the Galactic interstellar polarization from the reddening along each line of sight, using the extinction map of Schlafly & Finkbeiner (2011) and assuming  $R_V = 3.1$ . According to Serkowski et al. (1975), the upper bound to the interstellar polarization is  $p_{\max}(\%) = 9E(B-V)$ , while a typical value for interstellar polarization is  $\sim 3E(B-V)$ . With a Galactic reddening of  $E(B-V) = 0.07$ , the expected foreground interstellar polarization for J224256 is  $\sim 0.2\%$  with a likely maximum value of  $0.6\%$ . Thus, the detected  $\sim 2\%$  continuum polarization cannot be entirely ascribed to Galactic interstellar polarization, and some polarization from the object itself is required, either from the AGN itself, from absorption or scattering within its close environment, or from interstellar absorption within the host galaxy. At the wavelengths of broad emission lines, the polarization is indistinguishable from the continuum polarization: for Mg II we find  $p = (2.5 \pm 0.8)\%$  over  $3940\text{--}4000 \text{ \AA}$  (in observed wavelength), and for H $\beta$  we find  $p = (2.2 \pm 0.3)\%$  (integrated over  $6830\text{--}6960 \text{ \AA}$ ).<sup>4</sup> Thus, there are no polarization features that would suggest the presence of a hidden broad-line region in this galaxy.

These results stand in marked contrast to those of Zakamska et al. (2005), who found much higher blue continuum polarizations of 3–17% in 9 out of 12 objects observed from the Z03 sample. For our sample, the polarization characteristics are much more consistent with the properties of Seyfert 1 galaxies, in which optical polarizations of  $\lesssim 1\%$  are typical and  $p$  rarely exceeds 2% (Smith et al. 2002). This suggests that the variability selection is picking out a subset of the parent sample having properties that are significantly different from the majority of Type 2 quasars that have been previously chosen for follow-up observations.

#### 4. NOTES ON INDIVIDUAL OBJECTS

Below, we describe features of the SDSS and Keck spectra and discuss the classification of each variable object.

*SDSS J005515.81–004648.5*: The SDSS data show the likely presence of a broad H $\alpha$  line at the red end of the spectrum, although it is very noisy. The LRISp spectrum confirms the presence of broad H $\alpha$  wings as well as a broad Mg II line. No broad wings are apparent on the H $\beta$  line, so this object would be best classified as a Type 1.9 AGN.

*SDSS J012925.82–005900.2*: This object has a definite Type 1 AGN spectrum, although it is unusual in that the [O III]  $\lambda\lambda 4959, 5007$  lines are fairly broad and blended together. Broad lines in the spectrum include H $\beta$ , H $\gamma$ , H $\delta$ , and Mg II. This object is included in the SDSS DR5 quasar catalog (Schneider et al. 2007).<sup>5</sup>

*SDSS J013801.57–004946.5*: Broad Mg II  $\lambda 2800$  is present at the noisy blue end of the SDSS spectrum.

*SDSS J013856.14+003437.4*: The source has fairly weak emission lines, and the S/N of the SDSS spectrum is too low to clearly distinguish whether a broad H $\beta$  component is present. It lies just barely above the  $5\sigma$  variability threshold for inclusion in our sample.

*SDSS J014657.23+005537.2*: Mg II is visible in the SDSS

<sup>4</sup> At wavelengths  $\gtrsim 9000 \text{ \AA}$  the polarization calibration becomes unreliable and we are unable to measure a robust polarization for the H $\alpha$  line.

<sup>5</sup> The SDSS DR8 archive server incorrectly assigns a redshift of  $z = 6.03$  to this object, due to misidentification of [O III] as Ly  $\alpha$ .

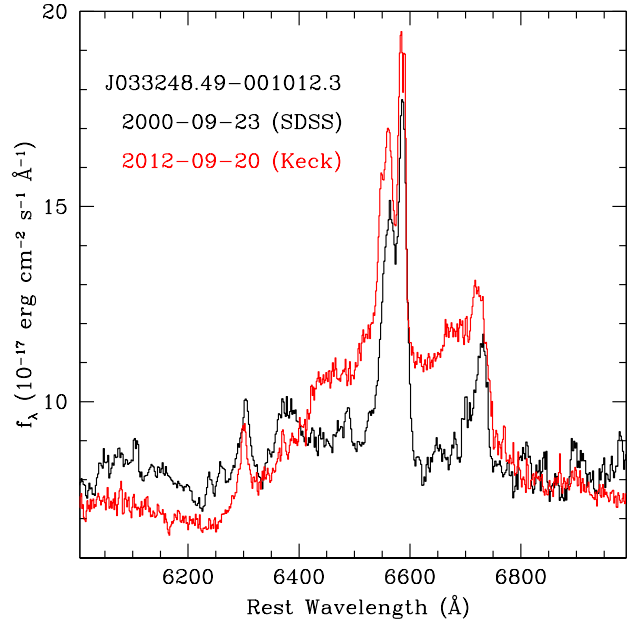


FIG. 7.— Comparison between the SDSS spectrum (smoothed by a 5-pixel boxcar) and the LRISp total flux spectrum (scaled by a factor of 0.67) for SDSS J033248.49–001012.3, illustrating the change in the broad H $\alpha$  profile over a 12-year span.

spectrum and appears broader than [O II] or [O III], but the S/N is fairly low.

*SDSS J023759.75+001723.5*: This source has a starlight-dominated spectrum with weak emission lines and possible weak broad bump at the wavelength of H $\alpha$ .

*SDSS J032011.94+002702.2*: This is another starlight-dominated source with weak emission lines. Broad Mg II is likely present at the blue end of the SDSS spectrum, and confirmed in the LRISp data. Broad H $\alpha$  wings are also visible in the LRISp spectrum, although the red-side data are noisy and impacted by night-sky emission-line residuals.

*SDSS J033123.14–005930.7*: This source has strong narrow emission lines and does not appear to have broad wings on the H $\beta$  emission line. However, a broad, very low-amplitude Mg II  $\lambda 2800$  line is possibly present.

*SDSS J033248.49–001012.3*: The SDSS spectrum initially appears consistent with a Type 2 AGN classification, with a starlight-dominated continuum. However, the LRISp spectrum reveals a strong and extremely broad H $\alpha$  emission line as well as broad Mg II, giving an appearance similar to typical double-peaked H $\alpha$  emitters (e.g., Strateva et al. 2003). Comparison between the SDSS and Keck spectra, taken 12 years apart, shows that the very broad H $\alpha$  feature was probably present but much weaker in the earlier data (Figure 7). The SDSS spectrum has a prominent bump at rest wavelength  $\sim 6400 \text{ \AA}$  and an extended “shelf” blueward of the narrow H $\alpha$  emission line, and the AGN was probably classified as a Type 2 quasar as a result of the relatively low amplitude of these broad features, as well as the lack of an obvious “normal” broad-line component. This object is also included in the SDSS quasar catalog (Schneider et al. 2007) and has been considered as a Type 1 AGN in other studies (Shen et al. 2008).

Of the seven objects having spectropolarimetry data, J033248 is the only one detected in the FIRST radio survey (Becker et al. 1995), where it is found to be a 15.7 mJy

TABLE 2  
CONTINUUM POLARIZATION

Object	$E(B-V)$ (mag)	$\lambda_{\text{obs}}$ (Å)	$p$ (%)	$\theta$ (deg)
J005515	0.03	4000–4900	$0.59 \pm 0.48$	$155 \pm 15$
J032011	0.09	4200–5300	$1.03 \pm 1.40$	...
J033248	0.10	4000–4800	$1.38 \pm 0.20$	$175 \pm 4$
J034252	0.11	4600–5200	$1.16 \pm 0.51$	$133 \pm 11$
J224256	0.07	4920–5230	$2.39 \pm 0.37$	$115 \pm 4$
J230612	0.05	4000–5300	$0.07 \pm 0.18$	...
J231845	0.04	4000–5300	$0.05 \pm 0.80$	...

NOTE. — Wavelength ranges for the polarization measurement are listed in the observed frame. Polarization angles are not reported for objects having continuum polarization consistent with zero. Galactic foreground reddening  $E(B-V)$  values are based on Schlafly & Finkbeiner (2011) and taken from NED, assuming  $R_V = 3.1$ . The maximum expected Galactic interstellar polarization is  $p_{\text{max}}(\%) \approx 9E(B-V)$  (Serkowski et al. 1975).

source. The deconvolved major and minor axis sizes are 1.77 and 0.91 arcsec, respectively, with the major axis oriented at  $\text{PA}=179.^\circ 6$ , nearly parallel to the optical polarization angle. Smith et al. (2004) interpret the relative orientation of the radio and optical polarization position angles in Type 1 AGNs as a consequence of the inclination angle of the AGN. In this picture (see also Marin et al. 2012), objects in which the optical polarization angle is parallel to the radio axis are viewed at relatively face-on inclinations ( $< 45^\circ$ ) and dominated by equatorial rather than polar scattering. The properties of this object appear consistent with this interpretation, although we caution that the observed polarization of 1.38% is only slightly larger than the maximum allowed Galactic interstellar polarization of  $\sim 1.0\%$ , which leaves open the possibility that the relative alignment of the radio and optical polarization axes could be substantially affected by the Galactic contribution.

*SDSS J034252.47+005252.4*: The SDSS spectrum appears consistent with a Type 2 classification, but the LRISp spectrum reveals broad Mg II, broad  $\text{H}\beta$  wings, and the blue half of a broad  $\text{H}\alpha$  line, cut off at the end of the red spectrum. This AGN appears in the SDSS DR5 quasar catalog (Schneider et al. 2007), and is included in both the Z03 and R08 samples.

*SDSS J222433.31–003634.0*: The SDSS spectrum is fairly noisy but appears consistent with a Type 2 classification.

*SDSS J223136.27–011045.0*: The SDSS spectrum shows a noisy broad bump at Mg II.

*SDSS J223959.04+005138.3*: A broad  $\text{H}\alpha$  line is likely present but is in the very noisy region at the red end of the SDSS spectrum.

*SDSS J224256.47+005155.2*: The SDSS spectrum shows strong narrow emission lines and a featureless continuum. Broad, blueshifted wings are present on the [O III] lines, while  $\text{H}\beta$  appears to have an extended red wing not present on [O III]. A weak, low-amplitude broad He II  $\lambda 4686$  emission line is also visible. Overall, the SDSS spectrum appears to be plausibly consistent with a Type 1 classification, albeit with relatively narrow and weak broad lines, and this source is included in the SDSS DR5 quasar catalog (Schneider et al. 2007). Figure 8 illustrates the profiles of several emission lines in the Keck LRISp spectrum. Although the blueshifted wings of [O II] and [O III] extends out to velocities beyond  $2000 \text{ km s}^{-1}$ , the Balmer lines have red wings extending to similarly high velocities while the forbidden oxygen lines

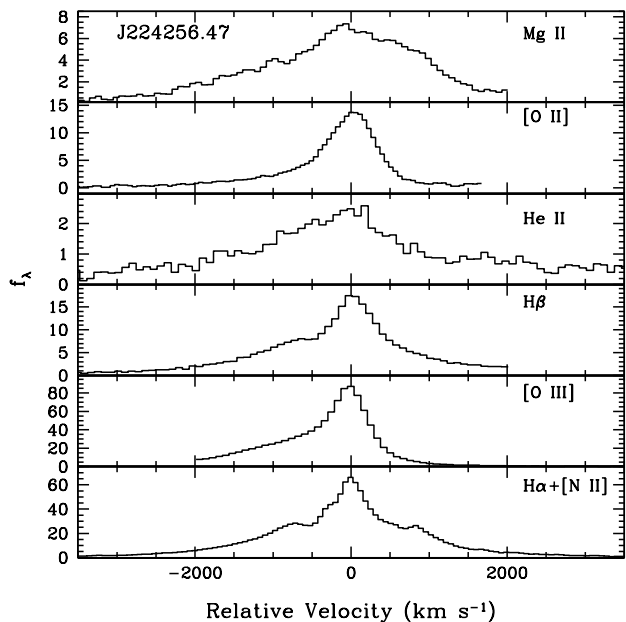


FIG. 8.— Comparison of line profiles for SDSS J224256.47+005155.2 in the Keck LRISp spectrum, illustrating broad permitted emission features as well as extended blue wings on the narrow emission lines.

do not. The contrast between the widths of Mg II ( $\text{FWHM} \approx 2400 \text{ km s}^{-1}$ ) and [O II] ( $\text{FWHM} \approx 880 \text{ km s}^{-1}$ ) gives the clearest indication that this is a Type 1 AGN.

Interestingly, SDSS J224256 has a spectrum that is overall extremely similar to that of IRAS 20181–2244, an object at  $z = 0.185$  that was originally classified as a Type 2 quasar by Elizalde & Steiner (1994). It was later demonstrated to be a Type 2 impostor by Halpern & Moran (1998) who detected broad wings on the Balmer lines and reclassified it as a narrow-line Seyfert 1 (NLS1) galaxy.<sup>6</sup>

*SDSS J225102.40–000459.8*: There is a low-amplitude, broad Mg II line in the SDSS spectrum.

<sup>6</sup> Halpern & Moran (1998) refer to IRAS 20181–2244 as a “I Zw 1”-type object because of the narrowness of its permitted broad lines, although it does not have the extremely strong Fe II emission that is a characteristic of I Zw 1 itself. Such objects are most often referred to as NLS1s, but they avoided that term in order to prevent confusion with narrow-line (i.e., obscured, Type 2) AGNs. Regardless of the terminology, SDSS J224256.47 and IRAS 20181–2244 have very similar spectra with definite broad Balmer-line components and other features that are consistent with a Type 1 classification.

*SDSS J230612.90–005912.6:* The spectrum contains strong narrow emission lines on a starlight-dominated continuum, giving the appearance of a Seyfert 2 galaxy. However, weak broad wings appear to be present on the  $H\alpha$  line, and this object was included in the Greene & Ho (2007) catalog of Type 1 AGNs with black hole mass estimates based on the broad  $H\alpha$  width. Broad Mg II and  $H\alpha$  wings are obvious in the Keck spectrum, and a low-amplitude broad  $H\beta$  feature is also visible.

*SDSS J231845.12–002951.4:* Broad Mg II and  $H\alpha$  are likely present at the blue and red ends of the SDSS spectrum, and are confirmed in the Keck spectrum.

## 5. DISCUSSION

As described in the Introduction, the simplest version of unified models for AGNs leads to a general expectation that optical variability should not be seen in Type 2 AGNs on timescales of a few years or less. While it is true that 90% of our SDSS sample is consistent with this prediction, the detection of variability in 10% of the Type 2 AGN population is surprising. We can consider several possible explanations for this finding.

*“Naked” or “true” Type 2 AGNs:* One possibility is that optical variability has been detected in unobscured AGNs that do not possess a BLR, similar to the so-called naked or true Type 2 AGNs identified by other means. X-ray spectroscopy and other observations have revealed a small number of candidates for unobscured Type 2 Seyfert galaxies showing no evidence for the presence of a BLR (e.g., Pappa et al. 2001; Boller et al. 2003; Wolter et al. 2005; Panessa et al. 2009; Shi et al. 2010; Tran et al. 2011; Bianchi et al. 2012; Gallo et al. 2013; Miniutti et al. 2013). The existence of such objects at very low luminosities can be understood in the context of disk-wind models that propose a lower bound in luminosity or in Eddington ratio ( $L/L_{\text{Edd}}$ ) below which the BLR would be unable to form (Nicastro 2000; Elitzur & Ho 2009; Trump et al. 2011). Alternatively, Laor (2003) proposed a luminosity threshold below which the BLR would have such small radius and such high Keplerian velocities that it could not remain stable. A more speculative question is whether unobscured Type 2 AGNs may exist at quasar-like luminosities (as proposed by Hawkins 2004) or at Eddington ratios well above the threshold at which the BLR is capable of forming. The existence of luminous, unobscured Type 2 AGNs above  $L/L_{\text{Edd}} \gtrsim 10^{-2}$  would require a different physical explanation than those proposed in the above scenarios (Gallo et al. 2013; Miniutti et al. 2013). Wang et al. (2012) recently described a time-dependent model in which the BLR is generated episodically from a star-forming accretion disk, and they predict that  $\sim 1\%$  of luminous AGNs would be observed during transient phases of weak or absent BLR emission, appearing as true Type 2 objects. More observational and theoretical effort is certainly needed to assess the possible existence of unobscured Type 2 quasars. However, in our SDSS sample, unobscured Type 2 AGNs are strongly disfavored as a primary explanation for optical variability, because the Keck observations revealed broad emission lines in each of the seven objects that were observed. High S/N spectroscopy of the remainder of our sample would be useful in order to test whether any other objects might still be candidate true Type 2 AGNs.

*Weak-lined quasars:* Surveys have detected a small population of unobscured AGNs whose broad emission lines are extremely weak (e.g., McDowell et al. 1995; Fan et al. 1999; Diamond-Stanic et al. 2009). The relationship between these

weak-lined quasars and true Type 2 AGNs is not entirely clear, partly because of the differences in selection methods. Weak-lined quasars have mainly been found at high redshift by identifying objects with a Lyman break but very little Ly  $\alpha$  or C IV emission, while true Type 2 AGN candidates are primarily low-redshift objects identified via their optical narrow-line emission. Could low-redshift counterparts of weak-lined quasars appear as Type 2 quasar impostors? Shemmer et al. (2010) presented infrared spectra of two high- $z$  weak-lined quasars, finding that they had extremely weak [O III] emission as well as very weak broad  $H\beta$  emission. If weak-lined quasars at lower redshift had similarly weak [O III] emission, they probably would not be included in optically-selected Type 2 quasar samples identified by their narrow-line emission. Although the data available to make this comparison are very sparse, the rest-frame optical spectra of high-redshift weak-lined quasars do not appear closely similar to the Z03 or R08 AGNs.

*Obscured AGNs visible in scattered light:* Obscured AGNs with hidden central engines visible in scattered light could exhibit some degree of variability, although the variability signal seen in scattered light would most likely be weak and temporally blurred by scattering over a spatially extended mirror. In this case, the timescale for significant variability could be used to constrain the size of the scattering region. Zakamska et al. (2005) examined *HST* images of three Type 2 quasars, finding evidence of kiloparsec-scale, conical scattering regions. If these sizes are typical of scattering regions in Type 2 quasars, then it would be unlikely that variability would be detected in the scattered light on timescales of a few years. We did not detect high polarization in any of the seven objects observed at Keck, and the spectropolarimetry results strongly disfavor the possibility that the detected variability in these AGNs is coming from a scattered light component.

*Changing appearance due to variable continuum luminosity:* Intermediate-type Seyferts (types 1.8 and 1.9) represent a “mixed bag” of AGNs having relatively weak broad emission lines due to either a low ionizing continuum flux, or extinction toward the BLR, or possibly both. Trippe et al. (2010) find that about half of a sample of local intermediate-type AGNs are classified as such due to a weak ionizing continuum. In such objects, significant fading of the continuum could make the BLR fade below detectability, giving the appearance of a Type 2 AGN but without significant obscuration. One example of this behavior is the highly variable AGN NGC 2992 (Trippe et al. 2008). Over the past few decades, this object has changed its appearance from Seyfert 1.5 to 1.9 to 2 primarily as a result of strong variations in the continuum luminosity, and not due to variable obscuration. (In a low state, such an object could be considered as an example of a temporarily naked Type 2 AGN.)

*State changes due to variable obscuration:* If an AGN was temporarily in a high-obscuration state when the SDSS spectrum was observed but the line-of-sight obscuration changed substantially during some portion of the Stripe 82 survey, the object could appear as a variable Type 2 AGN based on the available data. However, there are very few documented examples of AGNs changing from fully-obscured Type 2 states to unobscured Type 1 states; a possible example was presented by Aretxaga et al. (1999). More commonly, spectral variability in Type 1.8/1.9 AGNs due to variable obscuration can lead to dramatic changes in emission-line strength over timescales of years (Goodrich 1989, 1995). Halpern et al. (1998) discuss the instructive case of 1E 0449.4–1923, which

had previously been considered to be a Type 2 quasar candidate. They detected strong broad emission lines in this object and argued that the object was not a Type 2 quasar at all, but a partially obscured Type 1.8/1.9 object that emerged as a more obvious Type 1 AGN as a result of decreasing extinction toward the central engine. Such “variable intermediate-type AGNs” can easily be mistaken for Type 2 AGNs if they are observed when the obscuration is relatively high.

*Misclassification due to low S/N or incomplete spectral coverage:* The most trivial possibility would be that some of the variable Type 2 AGNs are simply Type 1 AGNs that were previously misclassified as a result of inadequate data quality in the original SDSS spectra, or some shortcoming in the sample selection procedure. Among the variable sources identified in this paper, only one object (SDSS J012925.81–005900.2) is an example of an obviously mistaken classification, but at least a handful of other objects seem to have probable or possible broad H $\alpha$  or Mg II features in the SDSS spectra that are too noisy to distinguish securely. The possibility of misclassification is exacerbated if an AGN happens to be in a faint state when observed spectroscopically, either due to variable obscuration or intrinsic flux variability. However, with sufficiently high S/N and spectral coverage that includes H $\alpha$  and/or Mg II, it should be possible to distinguish Type 1.8/1.9 AGNs from fully obscured Type 2 objects. In the past, some purported Type 2 quasars were found to be Type 1 objects after better data were obtained (Halpern & Moran 1998; Akiyama et al. 2002; Panessa et al. 2009; Gliozzi et al. 2010; Shi et al. 2010). The example of IRAS 20181–2244 (Halpern & Moran 1998) illustrates how tricky classification can be (similar to SDSS J224256.47+005155.2 discussed in this paper), because there are subclasses of Type 1 AGNs even at high luminosity that have very narrow permitted lines and can easily be mistaken for Type 2 objects.

*Other transient sources:* A supernova in a Type 2 AGN host galaxy could result in a spurious detection of AGN variability. However, such an event should in principle be identifiable as a supernova by its light curve shape, even if no contemporaneous spectrum was obtained. None of our detected variable sources has a light curve that appears consistent with a single supernova event.

For the sample discussed in this paper, the new Keck data easily clarify the situation. Out of seven objects observed at Keck, all seven are seen to be Type 1 AGNs, and the natural conclusion is that they were misclassified as Type 2 AGNs primarily because of low S/N and inadequate spectral coverage in the SDSS data. It seems likely that at least in some cases a contributing factor was that some AGNs may have been in a relatively faint state when the SDSS spectra were observed. For example, J033248 is seen to have very strongly double-peaked H $\alpha$  emission in the new Keck spectrum, but this feature is at most weakly present, if at all, in the earlier SDSS spectrum. Among the ten galaxies not having new Keck data, one is definitely a Type 1 AGN, and we identify possible weak broad emission lines in seven others based on examination of the SDSS data. Given that the Keck data had a 100% success rate for confirmation of possible or ambiguous broad lines that were seen in the SDSS data, it seems reasonable to extrapolate our results to conclude that the vast majority (and possibly all) of the variable sources are actually Type 1 AGNs. Based on the apparent weakness of H $\beta$  in the SDSS and Keck spectra, most of these appear to be variable “intermediate-type” 1.8 or 1.9 objects, similar to low-redshift AGNs previously identified as showing spectral variability (Goodrich 1989, 1995).

A larger fraction of our variable sources comes from the Z03 catalog than from the R08 catalog; we identify 13 variable Z03 objects in Stripe 82, but only six variable sources from the larger R08 sample (with two variable sources appearing in both samples). These were selected from a parent subsample of 89 Stripe 82 light curves for the Z03 sample, and 119 light curves for objects in the R08 sample (including 35 objects that overlap between the two). If we assume that all of the variable sources are misclassified Type 1 AGNs, this implies a contamination fraction of  $\sim 15\%$  for the Z03 sample, and  $\sim 5\%$  for the R08 sample. The lower contamination rate for R08 follows from their modified selection criteria, which are more efficient at excluding objects with weak broad lines. It would be straightforward to obtain new, high S/N spectroscopy of the remaining variable sources to test for the presence of broad emission lines, to determine whether *all* of the variable sources are Type 1 AGNs.

Overall, our results highlight the difficulty in identifying pure samples of Type 2 quasars by optical selection methods, echoing previous work by Halpern et al. (1998), Halpern & Moran (1998), Halpern et al. (1999), and others. Secure optical classifications of Type 2 AGNs require high S/N spectroscopy, and broad wavelength coverage can be critical. In particular, identifying AGNs as Type 2 objects based solely on H $\beta$  as the only BLR diagnostic line is particularly risky, in that broad H $\beta$  is often undetectably weak even in cases where broad H $\alpha$  wings or broad Mg II are quite obvious. Since our results indicate that all or nearly all variable “Type 2” quasars in Stripe 82 are actually Type 1 objects, future surveys could use optical variability as a criterion to exclude Type 1 contaminants from Type 2 AGN samples.

## 6. SUMMARY AND CONCLUSIONS

We have carried out a search for optical *g*-band variability among previously identified luminous Type 2 AGNs in SDSS Stripe 82, using image-subtraction photometry. Our conclusions can be summarized as follows.

1) No significant variability is found in the vast majority ( $\sim 90\%$ ) of the Z03 and R08 AGNs. This result is broadly consistent with the conclusions of Yip et al. (2009) who found no evidence of spectral variability in Type 2 AGNs, and is consistent with straightforward expectations for AGN unification models.

2) Among 173 AGNs for which light curves could be constructed, we found evidence of significant variability (above our  $5\sigma$  threshold) in 17 objects. Inspection of the SDSS spectra revealed possible or definite broad emission lines in several cases, suggesting that variability selection may be an efficient method for identifying Type 1 contaminants in Type 2 AGN samples.

3) Keck spectropolarimetry data were obtained for seven objects, none of which have high polarization, and all of which show broad emission lines in total flux.

4) Based on the available evidence, we conclude that most and possibly all of the variable AGNs in Z03 and R08 samples are actually Type 1 objects (mostly of Type 1.8/1.9) that contaminate Type 2 samples.

5) While we cannot rule out the possibility that a very small number of these variable AGNs might be unobscured Type 2 objects (“naked” AGNs), we conclude that it is much more likely that the variability selection is simply picking out misclassified Type 1 objects. Follow-up spectroscopy of the remaining variable AGNs would be useful to identify or rule out any remaining candidates for naked AGNs.

6) These results serve as a reminder of the difficulty in identifying pure samples of optically-selected Type 2 AGNs at high luminosity, although the small number of variable sources detected from the R08 catalog suggests a fairly low contamination fraction at a  $\sim 5\%$  level for this sample.

Research by A.J.B. and D.J.C. is supported by NSF grant AST-1108835. A.V. acknowledges support from the research grant RFFI 12-02-01358. We thank Shawn Thorman for his contributions to a preliminary version of this project. The work at LANL was supported by the Laboratory Directed Research and Development program. We thank the referee for helpful suggestions that improved this paper.

Funding for the SDSS and SDSS-II has been provided by the Alfred P. Sloan Foundation, the Participating Institutions, the National Science Foundation, the U.S. Department of Energy, the National Aeronautics and Space Administration, the Japanese Monbukagakusho, the Max Planck Society, and the Higher Education Funding Council for England. The SDSS Web Site is <http://www.sdss.org/>.

The SDSS is managed by the Astrophysical Research Consortium for the Participating Institutions. The Participating Institutions are the American Museum of Natural History, Astrophysical Institute Potsdam, University of Basel, University of Cambridge, Case Western Reserve University, University of Chicago, Drexel University, Fermilab, the Institute

for Advanced Study, the Japan Participation Group, Johns Hopkins University, the Joint Institute for Nuclear Astrophysics, the Kavli Institute for Particle Astrophysics and Cosmology, the Korean Scientist Group, the Chinese Academy of Sciences (LAMOST), Los Alamos National Laboratory, the Max-Planck-Institute for Astronomy (MPIA), the Max-Planck-Institute for Astrophysics (MPA), New Mexico State University, Ohio State University, University of Pittsburgh, University of Portsmouth, Princeton University, the United States Naval Observatory, and the University of Washington.

Some of the data presented herein were obtained at the W.M. Keck Observatory, which is operated as a scientific partnership among the California Institute of Technology, the University of California and the National Aeronautics and Space Administration. The Observatory was made possible by the generous financial support of the W.M. Keck Foundation. The authors wish to recognize and acknowledge the very significant cultural role and reverence that the summit of Mauna Kea has always had within the indigenous Hawaiian community. We are most fortunate to have the opportunity to conduct observations from this mountain. This research has made use of the NASA/IPAC Extragalactic Database (NED) which is operated by the Jet Propulsion Laboratory, California Institute of Technology, under contract with the National Aeronautics and Space Administration.

## REFERENCES

- Abazajian, K., Adelman-McCarthy, J. K., Agüeros, M. A., et al. 2003, *AJ*, 126, 2081
- Adelman-McCarthy, J. K., Agüeros, M. A., Allam, S. S., et al. 2008, *ApJS*, 175, 297
- Ai, Y. L., Yuan, W., Zhou, H. Y., et al. 2010, *ApJ*, 716, L31
- Akiyama, M., Ueda, Y., & Ohta, K. 2002, *ApJ*, 567, 42
- Alard, C., & Lupton, R. H. 1998, *ApJ*, 503, 325
- Antonucci, R. 2012, arXiv:1210.2716
- Antonucci, R. R. J., & Miller, J. S. 1985, *ApJ*, 297, 621
- Antonucci, R. 1993, *ARA&A*, 31, 473
- Aretxaga, I., Jöguet, B., Kunth, D., Melnick, J., & Terlevich, R. J. 1999, *ApJ*, 519, L123
- Barth, A. J., Filippenko, A. V., & Moran, E. C. 1999, *ApJ*, 525, 673
- Becker, R. H., White, R. L., & Helfand, D. J. 1995, *ApJ*, 450, 559
- Bershady, M. A., Trevese, D., & Kron, R. G. 1998, *ApJ*, 496, 103
- Bhatti, W. A., Richmond, M. W., Ford, H. C., & Petro, L. D. 2010, *ApJS*, 186, 233
- Bianchi, S., Panessa, F., Barcons, X., et al. 2012, *MNRAS*, 426, 3225
- Boller, T., Voges, W., Dennefeld, M., et al. 2003, *A&A*, 397, 557
- Butler, N. R., & Bloom, J. S. 2011, *AJ*, 141, 93
- Diamond-Stanic, A. M., Fan, X., Brandt, W. N., et al. 2009, *ApJ*, 699, 782
- Elitzur, M. 2012, *ApJ*, 747, L33
- Elitzur, M., & Ho, L. C. 2009, *ApJ*, 701, L91
- Elizalde, F., & Steiner, J. E. 1994, *MNRAS*, 268, L47
- Fan, X., Strauss, M. A., Gunn, J. E., et al. 1999, *ApJ*, 526, L57
- Gallo, L. C., MacMackin, C., Vasudevan, R., et al. 2013, *MNRAS*, 433, 421
- Gliozzi, M., Panessa, F., La Franca, F., et al. 2010, *ApJ*, 725, 2071
- Goodrich, R. W. 1989, *ApJ*, 340, 190
- Goodrich, R. W. 1995, *ApJ*, 440, 141
- Goodrich, R. W., Cohen, M. H., & Putney, A. 1995, *PASP*, 107, 179
- Greene, J. E., & Ho, L. C. 2007, *ApJ*, 667, 131
- Gu, M.-F., & Ai, Y. L. 2011, *A&A*, 528, A95
- Halpern, J. P., Eracleous, M., & Forster, K. 1998, *ApJ*, 501, 103
- Halpern, J. P., & Moran, E. C. 1998, *ApJ*, 494, 194
- Halpern, J. P., Turner, T. J., & George, I. M. 1999, *MNRAS*, 307, L47
- Hawkins, M. R. S. 2004, *A&A*, 424, 519
- Jia, J., Ptak, A., Heckman, T., & Zakamska, N. 2012, *ApJ*, submitted (arXiv:1205.0033)
- Laor, A. 2003, *ApJ*, 590, 86
- MacLeod, C. L., Ivezić, Ž., Kochanek, C. S., et al. 2010, *ApJ*, 721, 1014
- MacLeod, C. L., Brooks, K., Ivezić, Ž., et al. 2011, *ApJ*, 728, 26
- MacLeod, C. L., Ivezić, Ž., Sesar, B., et al. 2012, *ApJ*, 753, 106
- Marconi, A., Risaliti, G., Gilli, R., et al. 2004, *MNRAS*, 351, 169
- Marin, F., Goosmann, R. W., Gaskell, C. M., Porquet, D., & Dovčiak, M. 2012, *A&A*, 548, A121
- McDowell, J. C., Canizares, C., Elvis, M., et al. 1995, *ApJ*, 450, 585
- Meusinger, H., Hinze, A., & de Hoon, A. 2011, *A&A*, 525, A37
- Miller, J. S., Robinson, L. B., & Goodrich, R. W. 1988, in *Instrumentation for Ground-Based Optical Astronomy, Present and Future* (New York: Springer), 157
- Miniutti, G., Saxton, R. D., Rodríguez-Pascual, P. M., et al. 2013, *MNRAS*, 433, 1764
- Moran, E. C., Barth, A. J., Kay, L. E., & Filippenko, A. V. 2000, *ApJ*, 540, L73
- Mulchaey, J. S., Myshotzky, R. F., & Weaver, K. A. 1992, *ApJ*, 390, L69
- Nicastro, F. 2000, *ApJ*, 530, L65
- Oke, J. B., Cohen, J. G., Carr, M., et al. 1995, *PASP*, 107, 375
- Palanque-Delabrouille, N., Yèche, C., Myers, A. D., et al. 2011, *A&A*, 530, A122
- Panessa, F., & Bassani, L. 2002, *A&A*, 394, 435
- Panessa, F., Carrera, F. J., Bianchi, S., et al. 2009, *MNRAS*, 398, 1951
- Pappa, A., Georgantopoulos, I., Stewart, G. C., & Zezas, A. L. 2001, *MNRAS*, 326, 995
- Plotkin, R. M., Anderson, S. F., Brandt, W. N., et al. 2010, *ApJ*, 721, 562
- Pogge, R. W. 1988, *ApJ*, 328, 519
- Ramos Almeida, C., Levenson, N. A., Alonso-Herrero, A., et al. 2011, *ApJ*, 731, 92
- Reyes, R., Zakamska, N. L., Strauss, M. A., et al. 2008, *AJ*, 136, 2373 (R08)
- Rockosi, C., Stover, R., Kibrick, R., et al. 2010, *Proc. SPIE*, 7735,
- Schmidt, K. B., Marshall, P. J., Rix, H.-W., et al. 2010, *ApJ*, 714, 1194
- Sakata, Y., Morokuma, T., Minezaki, T., et al. 2011, *ApJ*, 731, 50
- Sarajedini, V. L., Koo, D. C., Phillips, A. C., et al. 2006, *ApJS*, 166, 69
- Schlaflly, E. F., & Finkbeiner, D. P. 2011, *ApJ*, 737, 103
- Schmidt, K. B., Rix, H.-W., Shields, J. C., et al. 2012, *ApJ*, 744, 147
- Schneider, D. P., Hall, P. B., Richards, G. T., et al. 2007, *AJ*, 134, 102
- Serkowski, K., Mathewson, D. S., & Ford, V. L. 1975, *ApJ*, 196, 261
- Sesar, B., Ivezić, Ž., Lupton, R. H., et al. 2007, *AJ*, 134, 2236
- Shemmer, O., Trakhtenbrot, B., Anderson, S. F., et al. 2010, *ApJ*, 722, L152
- Shen, Y., Greene, J. E., Strauss, M. A., Richards, G. T., & Schneider, D. P. 2008, *ApJ*, 680, 169
- Shi, Y., Rieke, G. H., Smith, P., et al. 2010, *ApJ*, 714, 115
- Smith, J. E., Young, S., Robinson, A., et al. 2002, *MNRAS*, 335, 773
- Smith, J. E., Robinson, A., Alexander, D. M., et al. 2004, *MNRAS*, 350, 140
- Strateva, I. V., Strauss, M. A., Hao, L., et al. 2003, *AJ*, 126, 1720

- Tran, H. D. 1995, *ApJ*, 440, 565  
Tran, H. D. 2001, *ApJ*, 554, L19  
Tran, H. D., Lyke, J. E., & Mader, J. A. 2011, *ApJ*, 726, L21  
Trippe, M. L., Crenshaw, D. M., Deo, R., & Dietrich, M. 2008, *AJ*, 135, 2048  
Trippe, M. L., Crenshaw, D. M., Deo, R. P., et al. 2010, *ApJ*, 725, 1749  
Trump, J. R., Impey, C. D., Kelly, B. C., et al. 2011, *ApJ*, 733, 60  
Véron-Cetty, M.-P., Joly, M., & Véron, P. 2004, *A&A*, 417, 515  
Vignali, C., Alexander, D. M., & Comastri, A. 2004, *MNRAS*, 354, 720  
Vignali, C., Alexander, D. M., & Comastri, A. 2006, *MNRAS*, 373, 321  
Voevodkin, A. 2011, arXiv:1107.4244  
Wang, J.-M., Du, P., Baldwin, J. A., et al. 2012, *ApJ*, 746, 137  
Wolter, A., Gioia, I. M., Henry, J. P., & Mullis, C. R. 2005, *A&A*, 444, 165  
Wu, X.-B., Wang, R., Schmidt, K. B., et al. 2011, *AJ*, 142, 78  
Yip, C. W., Connolly, A. J., Vanden Berk, D. E., et al. 2009, *AJ*, 137, 5120  
York, D. G., Adelman, J., Anderson, J. E., Jr., et al. 2000, *AJ*, 120, 1579  
Zakamska, N. L., Strauss, M. A., Krolik, J. H., et al. 2003, *AJ*, 126, 2125 (Z03)  
Zakamska, N. L., Strauss, M. A., Heckman, T. M., Ivezić, Ž., & Krolik, J. H. 2004, *AJ*, 128, 1002  
Zakamska, N. L., Schmidt, G. D., Smith, P. S., et al. 2005, *AJ*, 129, 1212  
Zakamska, N. L., Strauss, M. A., Krolik, J. H., et al. 2006, *AJ*, 132, 1496  
Zuo, W., Wu, X.-B., Liu, Y.-Q., & Jiao, C.-L. 2012, arXiv:1209.0524